Electronic Supplementary Material (ESI) for RSC Advances.

Supplementary Information

Two-dimensional polar metals in $KNbO_3/BaTiO_3$ superlattices: first-principle calculations

Gang Li[a], Huiyu Huang[a], Shaoqin Peng[a], Ying Xiong[b], Yongguang Xiao[a], Shaoan Yan[c], Yanwei Cao[d], Minghua Tang[a*], Zheng Li[a*]

[a]School of Materials Science and Engineering, Xiangtan University, Xiangtan, Hunan, 411105, China

[b]School of Mathematics and Computational Science, Xiangtan University, Xiangtan 411105, China

[c]School of Mechanical Engineering, Xiangtan University, Xiangtan 411105, China

[d]CAS Key Laboratory of Magnetic Materials and Devices, Ningbo Institute of Materials Technology and Engineering, Chinese Academy of Sciences, Ningbo, Zhejiang 315201, China

E-mail: tangminghua@xtu.edu.cn, lizheng@xtu.edu.cn

1. Band diagram analysis for the PP-type SL

For the PP-type SL, the band diagram is shown in Fig. S7. As compared to the NN-type SL, electrons generated by the polar discontinuity at the interface are difficult to transfer to BTO, whereas in a PP-type SL, holes are easily transferred to BTO regions because of the higher value of E_v of BTO than that of KNO. Since electrons are present at the interface of the KNO region, holes generated by the polar discontinuity are firstly recombined with electrons induced by the polarization discontinuity, then remaining holes continue to transfer into the interface of the BTO region and occupy the lower

valence bands until 0.5 h^+ is completely transferred. Thus holes are all distributed on the interface of the BTO region, forming an unstable 2DHG. Since holes are almost entirely contributed by p_x/p_y states, they cannot be redistributed by the polarization electric field. Because the valence band occupied by unstable holes in the interface of BTO is much lower than the E_v of inner BTO and KNO (the E_v of KNO is slightly smaller than that of BTO), those holes occupying lower valence bands need to move to higher valence bands to achieve electrostatic balance, thus holes on the interface would diffuse to the entire SL until the occupied valence bands (*i.e.*, E_F) align with those in the BTO and KNO (the hole distribution is symmetric along the middle layer of BTO (KNO) region, as shown in Fig. 7). Because E_v of KNO is slightly smaller than that of BTO, most of the holes are distributed in the BTO region (the 3D charge density of the PP-type SL as the background image in Fig. S7(b)), only part of holes are transferred to the KNO region, turning the initial downward band bending into upward band bending (the change of E_c (E_v) shown in Fig. S7(a,b)). The upward bending of the macroscopic averaged electrostatic potential at the interface can confirm this inference as shown in Fig. S7(c). In addition, the distribution of holes also affects the internal spatial distribution of ferroelectric distortions of the entire SL. Take the BTO region as an example, owing to the fact that positive and negative charges are distributed in the head and tail terminals of polarization, these existing holes will enhance the dipole of the right interface but screen the dipole of the left interface. Therefore, in the BTO or KNO region, the ferroelectric distortion pattern's increasing trend of the ferroelectric displacement is consistent with the polarization direction, and the concentration of holes determines the degree of the increased displacement(the variety of length of green arrow for the PP-type SL as shown in Fig. S7(b)).

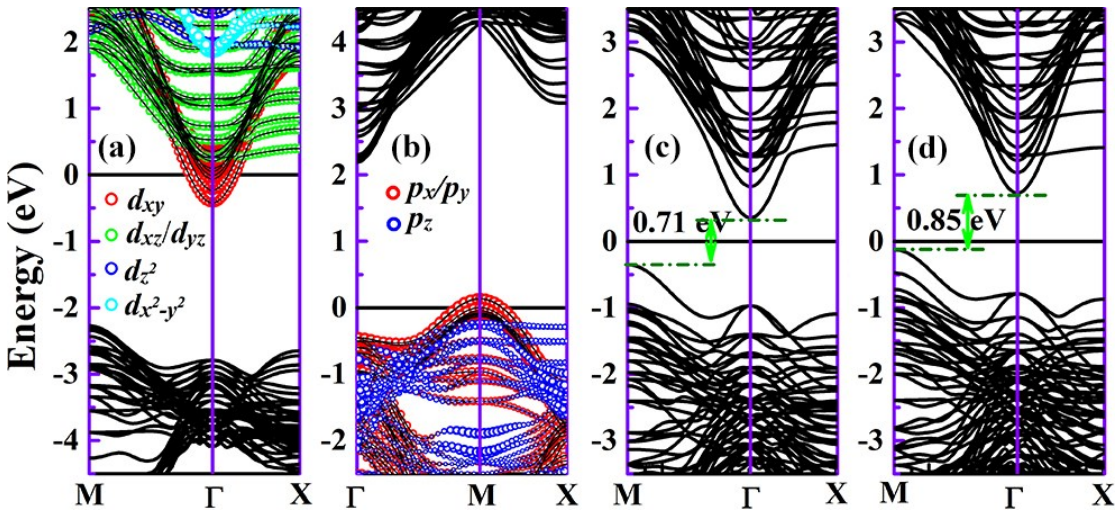

Fig. S1 Calculated electronic band structures for (a) NN-type, (b) PP-type, PN-type@P_{up}, PN-type@P_{dw} KNO/BTO SL, respectively.

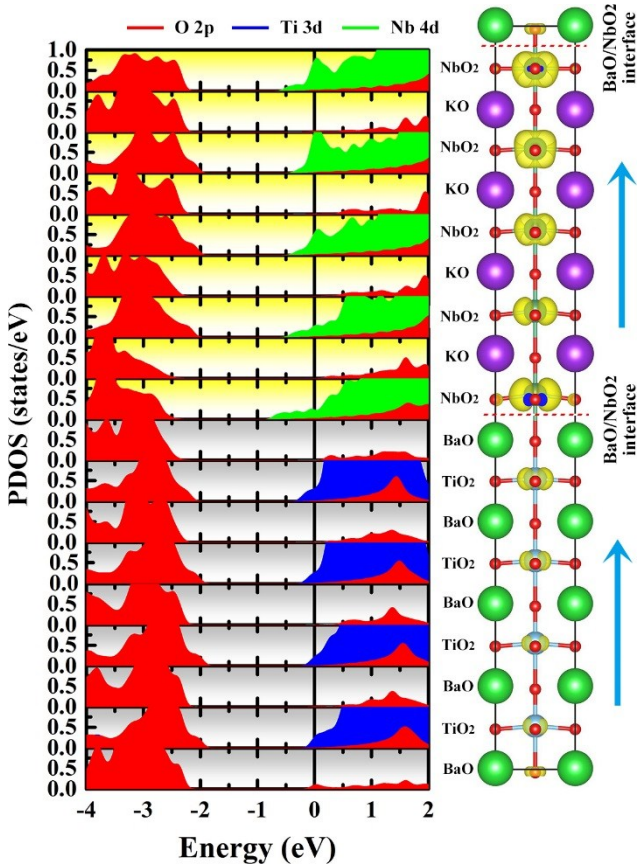

Fig. S2 Calculated layer-resolved partial DOS for the NN-type BTO/KNO SL when on-site Coulomb effective parameter values U=0 eV, along with its charge density plot projected on the bands forming the metallic states, the energy range from -1 to 0 eV.

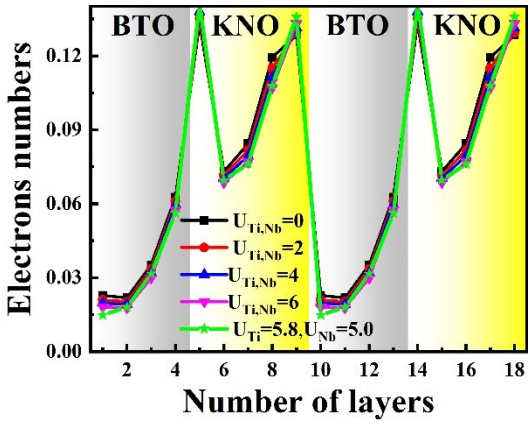

Fig. S3 Calculated layer-resolved total orbital electrons for each TiO_2 or NbO_2 layer in the NN-type SL under different on-site Coulomb effective U parameter values.

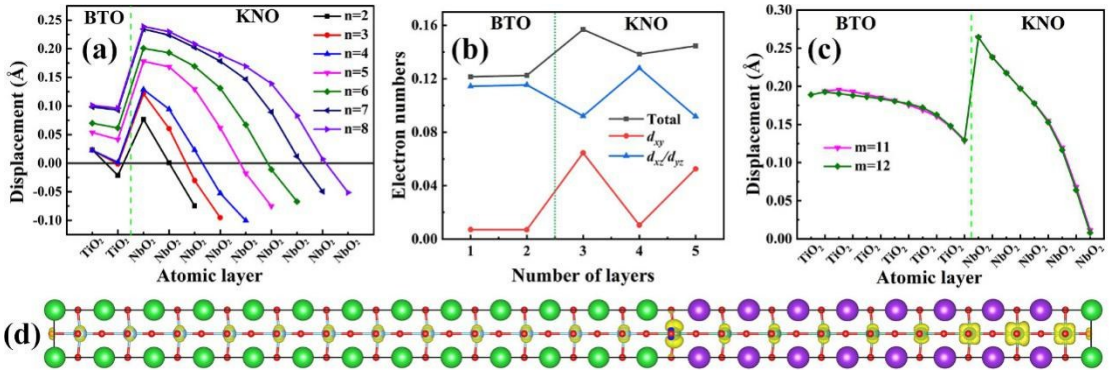

Fig. S4 (a) Calculated layer-resolved Ti-O (Nb-O) displacements of the NN-type SL with different n when fixed m=2. (b) Calculated the layer-resolved orbital electron distribution in the NN-type SL with m=2 and n=2. (c) Calculated layer-resolved Ti-O (Nb-O) displacements of the NN-type SL with m=11 (12) and n=8. (d) 3D charge density of NN-type SL with m=12 and n=8. The vertical green dotted line represents the interface. Here, the thickness of KNO and BTO are n and m (n, m=1, 2, 3, ···), respectively.

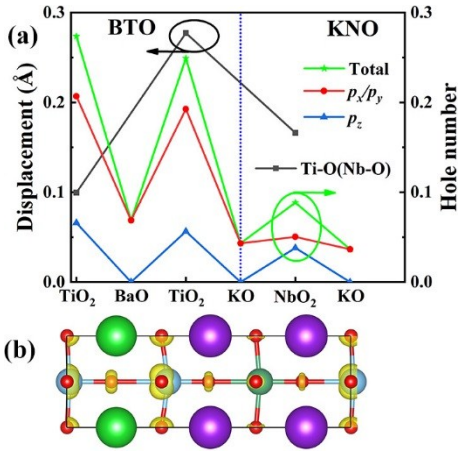

Fig. S5 Calculated layer-resolved Ti-O (Nb-O) displacement and hole number (a), 3D charge density (b) of PP-type SL with m=1 and n=1.

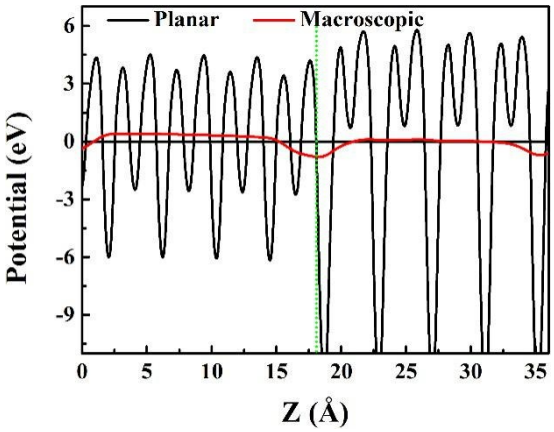

Fig. S6 Calculated planar and macroscopic averaged electrostatic potential of the NN-type SL along the *c*-axis, the green dot line indicates the interface. The left and right sides of the interface are the BTO and KNO regions, respectively.

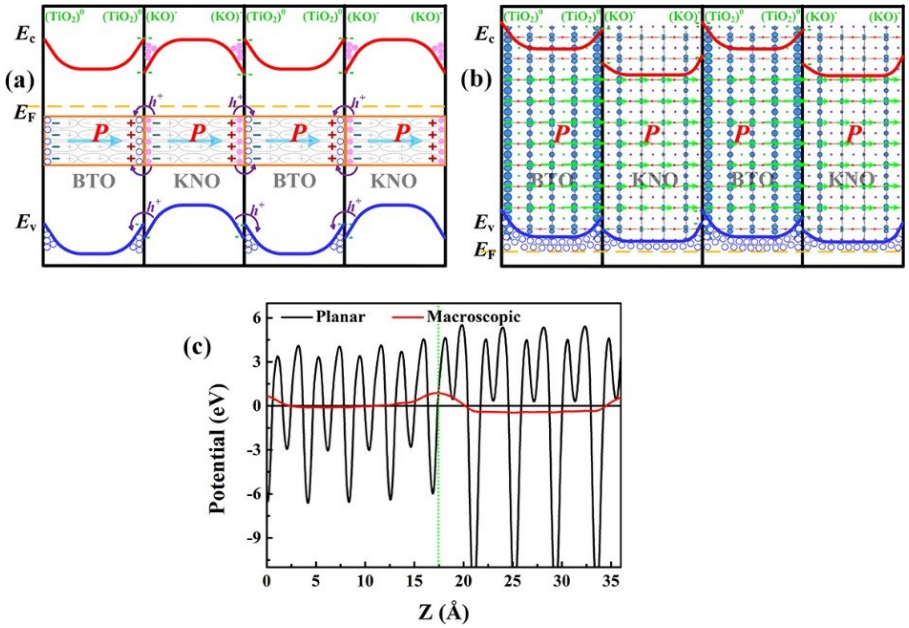

Fig. S7 (a) Band diagram for a PP-type SL after considered polarization, (b) the final band diagram for a PP-type SL; orange dashed line, red and blue thick solid line represent E_F, E_c, and E_v, separately. The pink and purple slim arrows represent the direction of electrons (pink solid circles) and holes (blue hollow circles) transfer, respectively, and light blue thick straight arrow indicates the direction of polarization. The green thin straight arrows represent the polarization of atomic layers, and its length is proportional to the magnitude of the displacement. (c) Calculated planar and macroscopic averaged electrostatic potential of the PP-type SL along the *c*-axis, the green dot line indicates the interface.

Tab. S1 The E_v, E_c, E_g of BTO and KNO, as well as the ΔE_v, ΔE_c, ΔE_g between of BTO and KNO at different on-site Coulomb effective U parameter values, where E_v of BTO used as a reference

	BTO			KNO			Δ(BTO-KNO)		
	E_v	E_c	E_g	E_v	E_c	E_g	ΔE_v	ΔE_c	ΔE_g
$U_{Ti,Nb}$=0	0	1.749	1.749	-0.152	1.396	1.548	0.152	0.353	0.201
$U_{Ti,Nb}$=1	0	1.869	1.869	-0.158	1.500	1.658	0.158	0.369	0.211
$U_{Ti,Nb}$=2	0	1.981	1.981	-0.146	1.624	1.770	0.146	0.357	0.211
$U_{Ti,Nb}$=3	0	2.103	2.103	-0.146	1.737	1.883	0.146	0.366	0.220
$U_{Ti,Nb}$=4	0	2.227	2.227	-0.148	1.857	2.005	0.148	0.370	0.222
$U_{Ti,Nb}$=5	0	2.368	2.368	-0.136	1.991	2.127	0.138	0.377	0.241
$U_{Ti,Nb}$=6	0	2.493	2.493	-0.141	2.112	2.253	0.141	0.381	0.245
$U_{Ti,Nb}$=7	0	2.638	2.638	-0.142	2.245	2.387	0.142	0.393	0.251
U_{Ti}=5.8 U_{Nb}=5.0	0	2.474	2.474	-0.155	1.972	2.127	0.155	-0.502	0.347